# Geometrically nonlinear analysis of thin-walled composite box beams

Thuc Phuong Vo* and Jaehong Lee†

*Department of Architectural Engineering, Sejong University*
*98 Kunja Dong, Kwangjin Ku, Seoul 143-747, Korea*

(Dated: August 25, 2008)

A general geometrically nonlinear model for thin-walled composite space beams with arbitrary lay-ups under various types of loadings has been presented by using variational formulation based on the classical lamination theory. The nonlinear governing equations are derived and solved by means of an incremental Newton-Raphson method. A displacement-based one-dimensional finite element model that accounts for the geometric nonlinearity in the von Kármán sense is developed. Numerical results are obtained for thin-walled composite box beam under vertical load to investigate the effect of geometric nonlinearity and address the effects of the fiber orientation, laminate stacking sequence, load parameter on axial-flexural-torsional response.

Keywords: thin-walled composites; classical lamination theory; axial-flexural-torsional response; nonlinear theory

## I. INTRODUCTION

Fiber-reinforced composite materials have been used over the past few decades in a variety of structures. Composites have many desirable characteristics, such as high ratio of stiffness and strength to weight, corrosion resistance and magnetic transparency. Thin-walled structural shapes made up of composite materials, which are usually produced by pultrusion, are being increasingly used in many engineering fields.

The theory of thin-walled closed section members made of isotropic materials was first developed by Vlasov [1] and Gjelsvik [2]. The large number of practical problems require a geometrically nonlinear formulation, such as the postbuckling behavior, load carrying capacity of structures used in aeronautical, aerospace as well as in mechanical and civil engineering. Within the formulation of this theory, the flexural displacements are assumed to be finite,

*Graduate student

†Professor, corresponding author. Tel.:+82-2-3408-3287; fax:+82-2-3408-3331

; Electronic address: jhlee@sejong.ac.kr

while the twist angle is taken to arbitrarily large. In the development of a geometrically nonlinear beam element, basically an updated Lagrangian or a total Lagrangian formulation can be employed. These formulations must be implemented using appropriate displacement interpolation functions. Bathe and Bolourchi [3] presented two consistent large rotation nonlinear three dimensional beam formulations: an updated Lagrangian and a total Lagrangian formulation for a 2-node Hermitian interpolation beam. Thin-walled composite structures are often very thin and have complicated material anisotropy. The studies of composite material carried out so far may broadly be divided into two groups. The first and most common approach is based on an analytical technique, while the other approach requires a two-dimensional finite element analysis to obtain the cross-section stiffness matrix. Atilgan and Hodges et al. [4,5] pioneered the second approach, which was referred to as the so-called "Variational Asymptotic Beam Section Analysis" (VABS). VABS used the variational asymptotic method (VAM) to split a three-dimensional nonlinear elasticity problem into a two-dimensional linear cross-sectional analysis and a one-dimensional, nonlinear beam problem. Hodges and co-workers (e.g., Cesnik et al. [6,7], Volovoi et al. [8], Yu et al. [9]) further applied the concept introduced by VAM to two dimensional cross-sectional problem and derived closed-form expressions for the cross-sectional stiffness coefficients of thin-walled beams. By using Atilgan and Hodges's beam model, Jeon et al. [10] developed an analysis model of large deflection for the static and dynamic analysis of composite box beams.

In the present investigation, an analytical approach is adopted for the derivation of the cross-sectional stiffness matrix considering different effects and their coupling to yield a general formulation. Bauld and Tzeng [11] presented nonlinear model for thin-walled composites by extending Gjelsvik's formulation to the balanced symmetric laminated composite materials. However, the formulation was somewhat not consistent in the sense that it used coordinate mapping when developing nonlinear stresses instead of variational formulation. A finite element formulation was developed by Stemple and Lee [12,13] to take into account the warping effect of composite beams undergoing large deflection or finite rotation. Kalfon and Rand [14] derived the nonlinear theoretical modeling of laminated thin-walled composite helicopter rotor blades. The derivation was based on nonlinear geometry with a detailed treatment of the body loads in the axial direction which were induced by the rotation. Pai and Nayfeh [15] developed a fully nonlinear theory of curved and twisted composite rotor blades. The theory accounted for warpings due to bending, extensional, shearing and torsional loadings, and three-dimensional stress effects by using the results of a two-dimensional, static, sectional, finite element analysis. Bhaskar and Librescu et al. [16,17] developed non-linear theory of composite thin-walled beams, which was employed in a broad field of engineering problems. In this model, the transverse shear deformation was taken into account but the warping torsion component was neglected. Special attention deserves the

works of Machado, Cortinez and Piovan [18,19,20] who introduced a geometrically non-linear theory for thin-walled composite beams for both open and closed cross-sections and took into account shear flexibility (bending and warping shear). This non-linear formulation was developed by using a non-linear displacement field, whose rotations were based on the rule of semi-tangential transformation. It was used for analyzing the stability of composite thin-walled beam with general cross-section. Recently, by using a geometrically higher-order non-linear beam theory, Machado [20] investigated the influence of large rotations on the buckling and free vibration behavior of thin-walled composite beam. However, it was strictly valid for symmetric balanced laminates and especially orthotropic laminates. A general geometrically nonlinear theory was derived by Lee [21] to study the lateral buckling of thin-walled composite beams with monosymmetric sections.

In the present paper, the analytical model developed by the authors [22] is extended to the geometric nonlinearity. A systematic approach based on the variational formulation is used to formulate the theory. A geometrically nonlinear model for thin-walled composite space beams with arbitrary laminate stacking sequences is given. The general nonlinear governing equations are derived and solved by means of an incremental Newton−Raphson method. Based on the analytical model, a displacement-based one-dimensional finite element model that accounts for the geometric nonlinearity in the von Kármán sense is developed. Numerical results are obtained for thin-walled composite box beam under vertical load to investigate the effect of geometric nonlinearity and address the effects of the fiber orientation, laminate stacking sequence, load parameter on axial-flexural-torsional response.

## II. KINEMATICS

The theoretical developments presented in this paper require two sets of coordinate systems which are mutually interrelated. The first coordinate system is the orthogonal Cartesian coordinate system $(x, y, z)$, for which the $x$ and $y$ axes lie in the plane of the cross section and the $z$ axis parallel to the longitudinal axis of the beam. The second coordinate system is the local plate coordinate $(n, s, z)$ as shown in Fig.1, wherein the $n$ axis is normal to the middle surface of a plate element, the $s$ axis is tangent to the middle surface and is directed along the contour line of the cross section. The $(n, s, z)$ and $(x, y, z)$ coordinate systems are related through an angle of orientation $\theta$ as defined in Fig.1. Point $P$ is called the pole axis, through which the axis parallel to the $z$ axis is called the pole axis.

To derive the analytical model for a thin-walled composite beam, the following assumptions are made:

1. The contour of the thin wall does not deform in its own plane.

2. The linear shear strain $\bar{\gamma}_{sz}$ of the middle surface is to have the same distribution in the contour direction as it does in the St. Venant torsion in each element.

3. The Kirchhoff-Love assumption in classical plate theory remains valid for laminated composite thin-walled beams.

According to assumption 1, the midsurface displacement components $\bar{u}, \bar{v}$ at a point $A$ in the contour coordinate system can be expressed in terms of a displacements $U, V$ of the pole $P$ in the $x, y$ directions, respectively, and the rotation angle $\Phi$ about the pole axis,

$$\bar{u}(s,z) = U(z)\sin\theta(s) - V(z)\cos\theta(s) - \Phi(z)q(s) \tag{1a}$$

$$\bar{v}(s,z) = U(z)\cos\theta(s) + V(z)\sin\theta(s) + \Phi(z)r(s) \tag{1b}$$

These equations apply to the whole contour. The out-of-plane shell displacement $\bar{w}$ can now be found from the assumption 2. For each element of middle surface, the shear strain become

$$\bar{\gamma}_{sz} = \frac{\partial \bar{v}}{\partial z} + \frac{\partial \bar{w}}{\partial s} = \Phi'(z)\frac{F(s)}{t(s)} \tag{2}$$

where $t(s)$ is thickness of contour box section, $F(s)$ is the St. Venant circuit shear flow. After substituting for $\bar{v}$ from Eq.(1) and considering the following geometric relations,

$$dx = ds\cos\theta \tag{3a}$$

$$dy = ds\sin\theta \tag{3b}$$

Eq.(2) can be integrated with respect to $s$ from the origin to an arbitrary point on the contour,

$$\bar{w}(s,z) = W(z) - U'(z)x(s) - V'(z)y(s) - \Phi'(z)\omega(s) \tag{4}$$

where differentiation with respect to the axial coordinate $z$ is denoted by primes ($'$); $W$ represents the average axial displacement of the beam in the $z$ direction; $x$ and $y$ are the coordinates of the contour in the $(x, y, z)$ coordinate system; and $\omega$ is the so-called sectorial coordinate or warping function given by

$$\omega(s) = \int_{s_\circ}^{s} \Big[r(s) - \frac{F(s)}{t(s)}\Big] ds \tag{5a}$$

$$\oint_i \frac{F(s)}{t(s)} ds = 2A_i \quad i = 1, ..., n \tag{5b}$$

where $r(s)$ is height of a triangle with the base $ds$; $A_i$ is the area circumscribed by the contour of the $i$ circuit. The explicit forms of $\omega(s)$ and $F(s)$ for box section are given in Ref.[22].

The displacement components $u, v, w$ representing the deformation of any generic point on the profile section are given with respect to the midsurface displacements $\bar{u}, \bar{v}, \bar{w}$ by the assumption 3.

$$u(s,z,n) = \bar{u}(s,z) \tag{6a}$$

$$v(s,z,n) = \bar{v}(s,z) - n\frac{\partial \bar{u}(s,z)}{\partial s} \tag{6b}$$

$$w(s,z,n) = \bar{w}(s,z) - n\frac{\partial \bar{u}(s,z)}{\partial z} \tag{6c}$$

The von Kármán type strains, in which only the products of $u, v$ and their derivatives are retained and all other nonlinear terms are neglected, are considered and given by

$$\epsilon_z = \frac{\partial w}{\partial z} + \frac{1}{2}\Big[\big(\frac{\partial u}{\partial z}\big)^2 + \big(\frac{\partial v}{\partial z}\big)^2\Big] \tag{7a}$$

$$\gamma_{sz} = \frac{\partial v}{\partial z} + \frac{\partial w}{\partial s} \tag{7b}$$

By substituting Eqs.(1), (4) and (6) into Eq.(7), and using the following relations

$$x - x_p = q\cos\theta + r\sin\theta \tag{8a}$$

$$y - y_p = q\sin\theta - r\cos\theta \tag{8b}$$

Eq.(7) can be rewritten as

$$\epsilon_z = \bar{\epsilon}_z + n\bar{\kappa}_z + n^2\bar{\chi}_z \tag{9a}$$

$$\gamma_{sz} = \bar{\gamma}_{sz} + n\bar{\kappa}_{sz} \tag{9b}$$

where

$$\bar{\epsilon}_z = \frac{\partial \bar{w}}{\partial z} + \frac{1}{2}\Big[\big(\frac{\partial \bar{u}}{\partial z}\big)^2 + \big(\frac{\partial \bar{v}}{\partial z}\big)^2\Big] \tag{10a}$$

$$\bar{\kappa}_z = -\frac{\partial^2 \bar{u}}{\partial z^2} - 2\frac{\partial^2 \bar{u}}{\partial s \partial z}\frac{\partial \bar{v}}{\partial z} \tag{10b}$$

$$\bar{\kappa}_{sz} = -2\frac{\partial^2 \bar{u}}{\partial s \partial z} \tag{10c}$$

$$\bar{\chi}_z = \Big(\frac{\partial^2 \bar{u}}{\partial s \partial z}\Big)^2 \tag{10d}$$

In Eq.(10), $\bar{\epsilon}_z$, $\bar{\kappa}_z, \bar{\kappa}_{sz}$ and $\bar{\chi}_z$ are midsurface axial strain, biaxial curvature and high order curvature of the shell, respectively. The above shell strains can be converted to beam strain components by substituting Eqs.(1), (4) and

(6) into Eq.(10) as

$$\bar{\epsilon}_z = \epsilon_z^\circ + x\kappa_y + y\kappa_x + \omega\kappa_\omega \tag{11a}$$

$$\bar{\kappa}_z = \kappa_y \sin\theta - \kappa_x \cos\theta - \kappa_\omega q + 2\chi_z r \tag{11b}$$

$$\bar{\kappa}_{sz} = \kappa_{sz} \tag{11c}$$

$$\bar{\chi}_z = \chi_z \tag{11d}$$

where $\epsilon_z^\circ, \kappa_x, \kappa_y, \kappa_\omega, \kappa_{sz}$ and $\chi_z$ are axial strain, biaxial curvatures in the $x$ and $y$ direction, warping curvature with respect to the shear center, twisting and high order curvature in the beam, respectively defined as

$$\epsilon_z^\circ = W' + \frac{1}{2}\left[U'^2 + V'^2 + (r^2+q^2)\Phi'^2\right] - x_p V'\Phi' + y_p U'\Phi' \tag{12a}$$

$$\kappa_x = -V'' - U'\Phi' \tag{12b}$$

$$\kappa_y = -U'' + V'\Phi' \tag{12c}$$

$$\kappa_\omega = -\Phi'' \tag{12d}$$

$$\kappa_{sz} = 2\Phi' \tag{12e}$$

$$\chi_z = \frac{1}{2}\Phi'^2 \tag{12f}$$

The resulting strains can be obtained from Eqs.(9) and (11) as

$$\epsilon_z = \epsilon_z^\circ + (x + n\sin\theta)\kappa_y + (y - n\cos\theta)\kappa_x + (\omega - nq)\kappa_\omega + (2rn + n^2)\chi_z \tag{13a}$$

$$\gamma_{sz} = (n + \frac{F}{2t})\kappa_{sz} \tag{13b}$$

## III. VARIATIONAL FORMULATION

Total potential energy of the system is calculated by sum of strain energy and the work done by external forces

$$\Pi = \mathcal{U} + \mathcal{V} \tag{14}$$

where $\mathcal{U}$ is the strain energy

$$\mathcal{U} = \frac{1}{2}\int_v (\sigma_z \epsilon_z + \sigma_{sz}\gamma_{sz}) dv \tag{15}$$

The variation of strain energy is calculated by substituting Eq.(13) into Eq.(15)

$$\begin{aligned}\delta\mathcal{U} &= \int_v \left\{\sigma_z\left[\delta\epsilon_z^\circ + (x + n\sin\theta)\delta\kappa_y + (y - n\cos\theta)\delta\kappa_x + (\omega - nq)\delta\kappa_\omega + (2rn + n^2)\delta\chi_z\right] + \sigma_{sz}(n + \frac{F}{2t})\delta\kappa_{sz}\right\} dv \\ &= \int_0^l (N_z\delta\epsilon_z^\circ + M_y\delta\kappa_y + M_x\delta\kappa_x + M_\omega\delta\kappa_\omega + M_t\delta\kappa_{sz} + R_z\delta\chi_z) ds \end{aligned} \tag{16}$$

where $N_z, M_x, M_y, M_\omega, M_t, R_z$ are axial force, bending moments in the $x$ and $y$ directions, warping moment (bi-moment), torsional moment and high order stress resultant with respect to the centroid respectively, defined by integrating over the cross-sectional area $A$ as

$$N_z = \int_A \sigma_z ds dn \tag{17a}$$

$$M_y = \int_A \sigma_z (x + n\sin\theta) ds dn \tag{17b}$$

$$M_x = \int_A \sigma_z (y - n\cos\theta) ds dn \tag{17c}$$

$$M_\omega = \int_A \sigma_z (\omega - nq) ds dn \tag{17d}$$

$$M_t = \int_A \sigma_{sz} (n + \frac{F}{2t}) ds dn \tag{17e}$$

$$R_z = \int_A \sigma_z (2rn + n^2) ds dn \tag{17f}$$

After substituting Eqs.(12) and (13) into Eq.(16), the variation of the strain energy can be obtained

$$\begin{aligned}\delta\mathcal{U} = \int_0^l \Big[ & N_z\delta W' - M_y\delta U'' - M_x\delta V'' - M_\omega\delta\Phi'' + 2M_t\delta\Phi' + N_z(U'\delta U' + V'\delta V') \\ + & (M_y - x_p N_z)(V'\delta\Phi' + \Phi'\delta V') - (M_x - y_p N_z)(U'\delta\Phi' + \Phi'\delta U') + (r_p^2 N_z + R_z)\Phi'\delta\Phi' \Big] dz\end{aligned} \tag{18}$$

On the other hand, the variation of work done by external forces can be written as

$$\delta\mathcal{V} = -\int_v (p_z\delta w + p_n\delta u + p_s\delta v) dv \tag{19}$$

where $p_z, p_n, p_s$ are forces acting in $z, n$ and $s$ direction. The above expression can be written with respect to the shell forces and displacements by using Eq.(6)

$$\delta\mathcal{V} = -\int_s\int_0^l (\bar{p}_z\delta\bar{w} + \bar{p}_n\delta\bar{n} + \bar{p}_s\delta\bar{v} - \bar{m}_z\frac{\partial\delta\bar{u}}{\partial z} - \bar{m}_s\frac{\partial\delta\bar{u}}{\partial s}) ds dz \tag{20}$$

where $\bar{p}_z, \bar{p}_s, \bar{m}_z, \bar{m}_s, \bar{p}_n$ are shell forces defined by

$$(\bar{p}_z, \bar{m}_z) = \int_n p_z(1, n) dn \tag{21a}$$

$$(\bar{p}_s, \bar{m}_s) = \int_n p_s(1, n) dn \tag{21b}$$

$$\bar{p}_n = \int_n p_n dn \tag{21c}$$

After substituting Eqs.(1) and (4) into Eq.(20), the variation of the work done by the external forces can be written with respect to the bar forces

$$\delta\mathcal{V} = -\int_0^l [\mathcal{P}_z\delta W + \mathcal{V}_x\delta U + \mathcal{M}_y\delta U' + \mathcal{V}_y\delta V + \mathcal{M}_x\delta V' + \mathcal{T}\delta\Phi + \mathcal{M}_\omega\delta\Phi'] dz \tag{22}$$

where the bar forces are related to the shell forces as

$$\mathcal{P}_z = \int_s \bar{p}_z ds \tag{23a}$$

$$\mathcal{V}_y = \int_s (\bar{p}_s \sin\theta - \bar{p}_n \cos\theta) ds \tag{23b}$$

$$\mathcal{V}_x = \int_s (\bar{p}_s \cos\theta + \bar{p}_n \sin\theta) ds \tag{23c}$$

$$\mathcal{T} = \int_s (\bar{p}_s r - \bar{p}_n q + \bar{m}_s) ds \tag{23d}$$

$$\mathcal{M}_y = \int_s (\bar{m}_z \sin\theta - \bar{p}_z x) ds \tag{23e}$$

$$\mathcal{M}_x = \int_s (\bar{m}_z \cos\theta - \bar{p}_z y) ds \tag{23f}$$

$$\mathcal{M}_\omega = \int_s (\bar{m}_z q - \bar{p}_z \omega) ds \tag{23g}$$

Principle of total potential energy can be stated as

$$0 = \delta\Pi = \delta\mathcal{U} + \delta\mathcal{V} \tag{24}$$

Substituting Eqs.(18) and (22) into Eq.(24), the weak form of the present theory for thin-walled composite beams are given by

$$\begin{aligned} 0 = & \int_0^l \Big[ N_z \delta W' - M_y \delta U'' - M_x \delta V'' - M_\omega \delta\Phi'' + 2M_t \delta\Phi' + N_z (U'\delta U' + V'\delta V') \\ & + (M_y - x_p N_z)(V'\delta\Phi' + \Phi'\delta V') - (M_x - y_p N_z)(U'\delta\Phi' + \Phi'\delta U') + (r_p^2 N_z + R_z)\Phi'\delta\Phi' \\ & - \mathcal{P}_z \delta W - \mathcal{V}_x \delta U - \mathcal{M}_y \delta U' - \mathcal{V}_y \delta V - \mathcal{M}_x \delta V' - \mathcal{T}\delta\Phi - \mathcal{M}_\omega \delta\Phi' \Big] dz \end{aligned} \tag{25}$$

## IV. CONSTITUTIVE EQUATIONS

The constitutive equations of a $k^{th}$ orthotropic lamina in the laminate co-ordinate system are given by

$$\begin{Bmatrix} \sigma_z \\ \sigma_{sz} \end{Bmatrix}^k = \begin{bmatrix} \bar{Q}^*_{11} & \bar{Q}^*_{16} \\ \bar{Q}^*_{16} & \bar{Q}^*_{66} \end{bmatrix}^k \begin{Bmatrix} \epsilon_z \\ \gamma_{sz} \end{Bmatrix} \tag{26}$$

where $\bar{Q}^*_{ij}$ are transformed reduced stiffnesses. The transformed reduced stiffnesses can be calculated from the transformed stiffnesses based on the plane stress ($\sigma_s = 0$) and plane strain ($\epsilon_s = 0$) assumption. More detailed explanation can be found in Ref.[23].

The constitutive equations for bar forces and bar strains are obtained by using Eqs.(13), (17) and (26)

$$\begin{Bmatrix} N_z \\ M_y \\ M_x \\ M_\omega \\ M_t \\ R_z \end{Bmatrix} = \begin{bmatrix} E_{11} & E_{12} & E_{13} & E_{14} & E_{15} & E_{16} \\ & E_{22} & E_{23} & E_{24} & E_{25} & E_{26} \\ & & E_{33} & E_{34} & E_{35} & E_{36} \\ & & & E_{44} & E_{45} & E_{46} \\ & & & & E_{55} & E_{56} \\ \text{sym.} & & & & & E_{66} \end{bmatrix} \begin{Bmatrix} \epsilon_z^\circ \\ \kappa_y \\ \kappa_x \\ \kappa_\omega \\ \kappa_{sz} \\ \chi_z \end{Bmatrix} \tag{27}$$

where $E_{ij}$ are stiffnesses of the thin-walled composite, and can be defined by

$$E_{11} = \int_s A_{11} ds \tag{28a}$$

$$E_{12} = \int_s (A_{11}x + B_{11}\sin\theta) ds \tag{28b}$$

$$E_{13} = \int_s (A_{11}y - B_{11}\cos\theta) ds \tag{28c}$$

$$E_{14} = \int_s (A_{11}\omega - B_{11}q) ds \tag{28d}$$

$$E_{15} = \int_s (A_{16}\frac{F}{2t} + B_{16}) ds \tag{28e}$$

$$E_{16} = \int_s (2B_{11}r + D_{11}) ds \tag{28f}$$

$$E_{22} = \int_s (A_{11}x^2 + 2B_{11}x\sin\theta + D_{11}\sin^2\theta) ds \tag{28g}$$

$$E_{23} = \int_s \Big[A_{11}xy + B_{11}(y\sin\theta - x\cos\theta) - D_{11}\sin\theta\cos\theta\Big] ds \tag{28h}$$

$$E_{24} = \int_s \Big[A_{11}x\omega + B_{11}(\omega\sin\theta - qx) - D_{11}q\sin\theta\Big] ds \tag{28i}$$

$$E_{25} = \int_s \Big[A_{16}\frac{F}{2t}x + B_{16}(x + \frac{F\sin\theta}{2t}) + D_{16}\sin\theta\Big] ds \tag{28j}$$

$$E_{26} = \int_s \Big[2B_{11}rx + D_{11}(x + 2r\sin\theta) + F_{11}\sin\theta\Big] ds \tag{28k}$$

$$E_{33} = \int_s (A_{11}y^2 - 2B_{11}y\cos\theta + D_{11}\cos^2\theta) ds \tag{28l}$$

$$E_{34} = \int_s \Big[A_{11}y\omega - B_{11}(\omega\cos\theta + qy) + D_{11}q\cos\theta\Big] ds \tag{28m}$$

$$E_{35} = \int_s \Big[A_{16}\frac{F}{2t}y + B_{16}(y - \frac{F\cos\theta}{2t}) - D_{16}\cos\theta\Big] ds \tag{28n}$$

$$E_{36} = \int_s \Big[2B_{11}ry + D_{11}(y - 2r\cos\theta) - F_{11}\cos\theta\Big] ds \tag{28o}$$

$$E_{44} = \int_s (A_{11}\omega^2 - 2B_{11}\omega q + D_{11}q^2) ds \tag{28p}$$

$$E_{45} = \int_s \Big[A_{16}\frac{F}{2t}\omega + B_{16}(\omega - \frac{Fq}{2t}) - D_{16}q\Big] ds \tag{28q}$$

$$E_{46} = \int_s \Big[2B_{11}r\omega + D_{11}(\omega - 2rq) - F_{11}q\Big] ds \tag{28r}$$

$$E_{55} = \int_s (A_{66}\frac{F^2}{4t^2} + B_{66}\frac{F}{t} + D_{66})ds \tag{28s}$$

$$E_{56} = \int_s \Big[2B_{16}r\frac{F}{2t} + D_{16}(\frac{F}{2t} + 2r) - F_{16}\Big]ds \tag{28t}$$

$$E_{66} = \int_s (4D_{11}r^2 + 4rF_{11} + H_{11})ds \tag{28u}$$

where $A_{ij}, B_{ij}, D_{ij}$ matrices are extensional, coupling, bending stiffness and $F_{ij}, H_{ij}$ matrices are higher order stiffnesses, respectively, defined by

$$(A_{ij}, B_{ij}, D_{ij}, F_{ij}, H_{ij}) = \int \bar{Q}_{ij}(1, n, n^2, n^3, n^4)dn \tag{29}$$

It appears that the laminate stiffnesses $E_{ij}$ depend on the cross section of the composite beam. The explicit forms of the laminate stiffnesses $E_{ij}$ for composite box section are given in the Appendix A.

## V. GOVERNING EQUATIONS

The nonlinear equilibrium equations of the present study can be obtained by integrating the derivatives of the varied quantities by parts and collecting the coefficients of $\delta W, \delta U, \delta V$ and $\delta\Phi$

$$N_z' + \mathcal{P}_z = 0 \tag{30a}$$

$$M_y'' + [N_z(U' + y_p\Phi')]' - [M_x\Phi']' + \mathcal{V}_x - \mathcal{M}_y' = 0 \tag{30b}$$

$$M_x'' + [N_z(V' - x_p\Phi')]' + [M_y\Phi']' + \mathcal{V}_y - \mathcal{M}_x' = 0 \tag{30c}$$

$$M_\omega'' + 2M_t' + [N_z(r_p^2\Phi' + y_pU' - x_pV')]' + [M_yV']' - [M_xU']' + [R_z\Phi']' + \mathcal{T} - \mathcal{M}_\omega' = 0 \tag{30d}$$

The natural boundary conditions are of the form

$$\delta W : N_z \tag{31a}$$

$$\delta U : M_y' + N_z(U' + y_p\Phi') - M_x\Phi' \tag{31b}$$

$$\delta U' : M_y \tag{31c}$$

$$\delta V : M_x' + N_z(V' - x_p\Phi') + M_y\Phi' \tag{31d}$$

$$\delta V' : M_x \tag{31e}$$

$$\delta\Phi : M_\omega' + 2M_t + N_z(r_p^2\Phi' + y_pU' - x_pV') + M_yV' - M_xU' + R_z\Phi' \tag{31f}$$

$$\delta\Phi' : M_\omega \tag{31g}$$

The $7^{th}$ denotes the warping restraint boundary condition. When the warping of the cross section is restrained, $\Phi' = 0$ and when the warping is not restrained (free warping), $M_\omega = 0$. Eq.(30) is the general nonlinear equilibrium equations. In general, moment loads are not considered in the analysis ($\mathcal{M}_x = \mathcal{M}_y = \mathcal{M}_\omega = 0$).

By substituting Eqs.(12) and (27) into Eq.(30), the explicit form of the governing equations can be expressed with respect to the laminate stiffnesses $E_{ij}$ as

$$\begin{aligned}
&\left[E_{11}\left[W' + \frac{1}{2}\left[U'^2 + V'^2 + (r^2+q^2)\Phi'^2\right] - x_p V'\Phi' + y_p U'\Phi'\right] - E_{12}(U'' - V'\Phi')\right.\\
&\qquad\left. - E_{13}(V'' + U'\Phi') - E_{14}\Phi''' + 2E_{15}\Phi'' + \frac{1}{2}E_{16}\Phi'^2\right]' + \mathcal{P}_z = 0 \qquad (32a)\\
&\left[E_{12}\left[W' + \frac{1}{2}\left[U'^2 + V'^2 + (r^2+q^2)\Phi'^2\right] - x_p V'\Phi' + y_p U'\Phi'\right] - E_{22}(U'' - V'\Phi')\right.\\
&\qquad\left. - E_{23}(V'' + U'\Phi') - E_{24}\Phi'' + 2E_{25}\Phi'' + \frac{1}{2}E_{26}\Phi'^2\right]''\\
&+\left\{\left[E_{11}\left[W' + \frac{1}{2}\left[U'^2 + V'^2 + (r^2+q^2)\Phi'^2\right] - x_p V'\Phi' + y_p U'\Phi'\right] - E_{12}(U'' - V'\Phi')\right.\right.\\
&\qquad\left.\left. - E_{13}(V'' + U'\Phi') - E_{14}\Phi'' + 2E_{15}\Phi'' + \frac{1}{2}E_{16}\Phi'^2\right](U' + y_p\Phi')\right\}'\\
&-\left\{\left[E_{13}\left[W' + \frac{1}{2}\left[U'^2 + V'^2 + (r^2+q^2)\Phi'^2\right] - x_p V'\Phi' + y_p U'\Phi'\right] - E_{23}(U'' - V'\Phi')\right.\right.\\
&\qquad\left.\left. - E_{33}(V'' + U'\Phi') - E_{34}\Phi'' + 2E_{35}\Phi'' + \frac{1}{2}E_{36}\Phi'^2\right]\Phi'\right\}' + \mathcal{V}_x = 0 \qquad (32b)\\
&\left[E_{13}\left[W' + \frac{1}{2}\left[U'^2 + V'^2 + (r^2+q^2)\Phi'^2\right] - x_p V'\Phi' + y_p U'\Phi'\right] - E_{23}(U'' - V'\Phi')\right.\\
&\qquad\left. - E_{33}(V'' + U'\Phi') - E_{34}\Phi'' + 2E_{35}\Phi'' + \frac{1}{2}E_{36}\Phi'^2\right]''\\
&+\left\{\left[E_{11}\left[W' + \frac{1}{2}\left[U'^2 + V'^2 + (r^2+q^2)\Phi'^2\right] - x_p V'\Phi' + y_p U'\Phi'\right] - E_{12}(U'' - V'\Phi')\right.\right.\\
&\qquad\left.\left. - E_{13}(V'' + U'\Phi') - E_{14}\Phi'' + 2E_{15}\Phi'' + \frac{1}{2}E_{16}\Phi'^2\right](V' - x_p\Phi')\right\}'\\
&+\left\{\left[E_{12}\left[W' + \frac{1}{2}\left[U'^2 + V'^2 + (r^2+q^2)\Phi'^2\right] - x_p V'\Phi' + y_p U'\Phi'\right] - E_{22}(U'' - V'\Phi')\right.\right.\\
&\qquad\left.\left. - E_{23}(V'' + U'\Phi') - E_{24}\Phi'' + 2E_{25}\Phi'' + \frac{1}{2}E_{26}\Phi'^2\right]\Phi'\right\}' + \mathcal{V}_y = 0 \qquad (32c)\\
&\left[E_{14}\left[W' + \frac{1}{2}\left[U'^2 + V'^2 + (r^2+q^2)\Phi'^2\right] - x_p V'\Phi' + y_p U'\Phi'\right] - E_{24}(U'' - V'\Phi')\right.\\
&\qquad\left. - E_{34}(V'' + U'\Phi') - E_{44}\Phi'' + 2E_{45}\Phi'' + \frac{1}{2}E_{46}\Phi'^2\right]''
\end{aligned}$$

$$
\begin{aligned}
&+2\Bigg[E_{15}\Bigg[W'+\frac{1}{2}\big[U'^2+V'^2+(r^2+q^2)\Phi'^2\big]-x_pV'\Phi'+y_pU'\Phi'\Bigg]-E_{25}(U''-V'\Phi')\\
&\qquad -E_{35}(V''+U'\Phi')-E_{45}\Phi''+2E_{55}\Phi''+\frac{1}{2}E_{56}\Phi'^2\Bigg]'\\
&+\Bigg\{\Bigg[E_{11}\Bigg[W'+\frac{1}{2}\big[U'^2+V'^2+(r^2+q^2)\Phi'^2\big]-x_pV'\Phi'+y_pU'\Phi'\Bigg]-E_{12}(U''-V'\Phi')\\
&\qquad -E_{13}(V''+U'\Phi')-E_{14}\Phi''+2E_{15}\Phi''+\frac{1}{2}E_{16}\Phi'^2\Bigg](r_p^2\Phi'+y_pU'-x_pV')\Bigg\}'\\
&+\Bigg\{\Bigg[E_{12}\Bigg[W'+\frac{1}{2}\big[U'^2+V'^2+(r^2+q^2)\Phi'^2\big]-x_pV'\Phi'+y_pU'\Phi'\Bigg]-E_{22}(U''-V'\Phi')\\
&\qquad -E_{23}(V''+U'\Phi')-E_{24}\Phi''+2E_{25}\Phi''+\frac{1}{2}E_{26}\Phi'^2\Bigg]V'\Bigg\}'\\
&-\Bigg\{\Bigg[E_{13}\Bigg[W'+\frac{1}{2}\big[U'^2+V'^2+(r^2+q^2)\Phi'^2\big]-x_pV'\Phi'+y_pU'\Phi'\Bigg]-E_{23}(U''-V'\Phi')\\
&\qquad -E_{33}(V''+U'\Phi')-E_{34}\Phi''+2E_{35}\Phi''+\frac{1}{2}E_{36}\Phi'^2\Bigg]U'\Bigg\}'\\
&+\Bigg\{\Bigg[E_{16}\Bigg[W'+\frac{1}{2}\big[U'^2+V'^2+(r^2+q^2)\Phi'^2\big]-x_pV'\Phi'+y_pU'\Phi'\Bigg]-E_{26}(U''-V'\Phi')\\
&\qquad -E_{36}(V''+U'\Phi')-E_{46}\Phi''+2E_{56}\Phi''+\frac{1}{2}E_{66}\Phi'^2\Bigg]\Phi'\Bigg\}'+\mathcal{T} \;=\; 0
\end{aligned}
\tag{32d}
$$

Eq.(32) is most general form for axial-flexural-torsional behavior of a thin-walled composite beam, and the dependent variables $W$, $U$, $V$ and $\Phi$ are fully coupled.

## VI. FINITE ELEMENT FORMULATION

The present theory for thin-walled composite beams described in the previous section was implemented via a displacement based finite element method. The generalized displacements are expressed over each element as a combination of the one-dimensional linear Lagrange interpolation function $\Psi_j$ and Hermite-cubic interpolation function $\psi_j$ associated with node $j$ and the nodal values

$$W \;=\; \sum_{j=1}^{2} w_j\Psi_j \tag{33a}$$

$$U \;=\; \sum_{j=1}^{4} u_j\psi_j \tag{33b}$$

$$V \;=\; \sum_{j=1}^{4} v_j\psi_j \tag{33c}$$

$$\Phi \;=\; \sum_{j=1}^{4} \phi_j \psi_j \tag{33d}$$

Substituting these expressions into the weak statement in Eq.(25), the finite element model of a typical element can be expressed as

$$\big[K(\{\Delta\})\big]\{\Delta\} = \{f\} \tag{34}$$

The direct stiffness coefficients $K_{ij}^{\alpha\beta} = (K_{ij}^{\alpha\beta})_L + (K_{ij}^{\alpha\beta})_N$ are defined in the Appendix B. The nonlinear algebraic equations of present theory can be linearized using Newton−Raphson iterative method. Solution of Eq.(34) by the Newton−Raphson iteration method results in the following linearized equations for the incremental solution at the $r^{th}$ iteration (Bathe [24])

$$\big[T(\{\Delta\}^{r-1})\big]\{\delta\Delta\} = -\{R(\{\Delta\}^{r-1})\} \tag{35}$$

where the tangent stiffness matrix is calculated using the definition

$$\big[T(\{\Delta\}^{r-1})\big] \equiv \Big(\frac{\partial\{R\}}{\partial\{\Delta\}}\Big)^{r-1} \tag{36}$$

The residual vector vector after the $(r-1)^{th}$ iteration is given by

$$\{R(\{\Delta\}^{r-1})\} = [K(\{\Delta\}^{r-1})]\{\Delta\}^{r-1} - \{f\} \tag{37}$$

The solution at the $r^{th}$ iteration is then given by

$$\{\Delta\}^{r} = \{\Delta\}^{r-1} + \{\delta\Delta\} \tag{38}$$

The details of the direct stiffness matrix are given in the Appendix B. In Eq.(34), $\{\Delta\}$ is the unknown nodal displacements

$$\{\Delta\} = \{W\ U\ V\ \Phi\}^{\mathrm{T}} \tag{39}$$

## VII. NUMERICAL EXAMPLES

Throughout numerical examples, a tolerance of $\epsilon = 10^{-3}$ and maximum allowable iterations of 20 (per load step) are used to check for convergence of nodal displacements in the Newton−Raphson iteration scheme. The initial solution

vector is chosen to be the zero vector, so that the first iteration solution corresponds to the linear solution. The results of the present analysis are given for both the linear and nonlinear case.

For verification purpose, a cantilever composite box beam with geometry and stacking sequence shown in Fig.2 under a tip vertical load of 1.78 $kN$ is analyzed. The lamination of this beam consists of eight laminae of equal thickness as follows: $[0/-\theta_2/90]_s$ at the lower flange, $[0/\theta_2/90]_s$ at the upper flange and $[(0/90)_2]_s$ at both webs, respectively. The analysis is carried out assuming both plane stress ($\sigma_s = 0$) and plane strain ($\epsilon_s = 0$) assumptions. The following material properties are used (Stemple and Lee [12])

$$E_1 = 146.78\text{GPa}\,, E_2 = 10.3\text{GPa}\,, G_{12} = 6.2\text{GPa}\,, \nu_{12} = 0.28 \tag{40}$$

The vertical displacement and the angle of twist at the tip of the beam are plotted in Figs.3 and 4 with respect to fiber angle variation. It is shown that the vertical displacement more than doubles when fiber angle is varied from $\theta = 0^\circ$ to $\theta = 90^\circ$. It seems that the solutions in Stemple and Lee [12] and Kalfon and Rand [14] were calculated by using plane strain assumption. The axial and horizontal displacements with respect to fiber angle change are illustrated in Figs.5 and 6. These responses are due to coupling-induced geometrical nonlinear effect, which are not present in the linear analysis. The maximum coupling of this type is shown to be near fiber angle $\theta = 30^\circ$. The accuracy of the predictions from present model with Stemple and Lee [12] and Kalfon and Rand [14] can be seen. The proposed model agrees well with previously available results and can capture exactly all the geometrical nonlinear response of composite beam.

A pinned-hinged composite box beam of length $L = 8$m under an eccentric uniform load $q$ acting at the midplane of the left web is considered in order to investigate the effect of the load parameter and fiber orientation on the displacements. It is noted earlier by Lee [21,25] that the results based on the plane stress assumption ($\sigma_s = 0$) yield better agreement with ABAQUS solution. For this reason, plane stress assumption ($\sigma_s = 0$) is used in numerical computation. The geometry and stacking sequence of the composite box beam is shown in Fig.7, and the following engineering constants are used

$$E_1/E_2 = 25, G_{12}/E_2 = 0.6, \nu_{12} = 0.25 \tag{41}$$

For convenience, the following nondimensional values of the axial, vertical displacement, and load parameter are

used

$$\overline{w} = \frac{w}{b_1} \tag{42a}$$

$$\overline{v} = \frac{v}{b_1} \tag{42b}$$

$$\overline{q} = \frac{qL^4}{E_1 b_1^3 t_1} \tag{42c}$$

Stacking sequence of this beam consists of two layers with equal thickness as follows: $[\theta]_2$ at top flange and right web, $[-\theta]_2$ at left web and bottom flange, respectively (Fig.7). For this lay-up, most coupling stiffnesses become zero, but $E_{16}, E_{25}$ and $E_{35}$ do not vanish due to unsymmetric stacking sequence of the webs and flanges. Accordingly, this beam sustains simultaneously two kinds of couplings from material anisotropy and geometric nonlinearity.

As the first example, the stacking sequence at two specific fiber angle $\theta = 45°, 90°$ is considered to investigate the effects of load parameter on the displacements in the high nonlinear region. It should be noted that for $\theta = 90°$, all the coupling stiffness vanish, that is, only geometrical nonlinear effect exists. The load increment of $\Delta\bar{q} = 0.05$ is employed until the first critical point is reached. Figs.8 and 9 show the load versus vertical displacement and the load versus torsional displacement at two fiber angles. It is evident that the linear theory is adequate in a relatively large region up to the point where an applied load reaches value of $\bar{q} = 2$ and 4 for fiber angle $\theta = 90°$ and $45°$, respectively. When comparing with linear analysis, all the nonlinear displacements increase with increasing value of the load, except for the vertical displacement. This is due to the fact that the geometrical nonlinear effect causes axial-flexural-torsional coupling which results in an increase in the flexural stiffness and a decrease in the torsional stiffness of the beam. The effect of the geometric nonlinearity is apparent with increasing load intensity. The highest load of fiber angle $\theta = 90°$ is smaller than that of $\theta = 45°$. At this load, for $\theta = 45°$, the nonlinear vertical and torsional displacement is about 85% and 325% of the linear value, respectively. It is from Fig.10 that highlights the influence of geometrical nonlinear effect on the axial displacement of beam. This response is never seen in linear analysis because the coupling terms are not present. It implies that the structure under eccentric transverse load not only causes transverse displacement and angle of twist as would be observed in linear case, but also causes additional response due solely to geometric nonlinearity never seen in linear case.

To investigate the geometrical nonlinear effect further, the same configuration with the previous example except the load and the laminate stacking sequence is considered. A constant applied load is analyzed while the fiber angle is rotated in the webs and flanges. Based on previous numerical example, an applied load $\bar{q} = 5.0$ is chosen to show effect of fiber orientation on the axial-flexural-torsional response. Variation of the axial, vertical displacements with respect to fiber angle variation are plotted in Fig.11. As expected, no linear axial displacement $\bar{w}$ is seen for all fiber angle.

For fiber angles less than $\theta = 30°$, the vertical displacement of linear and nonlinear analysis coincides. Especially, in Fig.12, the angle of twist of two analyses shows the same tendency and reaches minimum value between fiber angle $\theta \in [20° - 30°]$, that is, because the torsional rigidity $E_{55}$ becomes maximum value at this range. However, as the fiber orientation is rotated off-axis, the geometrical nonlinear effect is prominent, that is, the discrepancy between the linear and nonlinear analysis becomes significant. It is observed that the nonlinear vertical displacement are not as sensitive as the nonlinear axial and torsional displacement when fiber angle changes. The difference between displacements of two analyses is minimum at $\theta = 0°$ and reaches maximum value at $\theta = 90°$. This phenomenon can be explained that the axial, flexural and torsional rigidities decrease significantly with increasing fiber angle, and thus, the relative geometrical nonlinear effect becomes larger for higher fiber angles.

## VIII. CONCLUDING REMARKS

A general geometrically nonlinear model for thin-walled composite space beams with arbitrary laminate stacking sequences under various types of loadings has been presented by using variational formulation based on the classical lamination theory. General nonlinear governing equations are derived from the principle of the stationary value of total potential energy and solved by means of an incremental Newton−Raphson method. A displacement-based one-dimensional finite element model that accounts for the geometric nonlinearity in the von Kármán sense is developed. Numerical results are obtained to investigate the effect of geometric nonlinearity on axial-flexural-torsional response, address the effects of fiber orientation, laminate stacking sequence and load parameter. The present model is found to be appropriate and efficient in analyzing geometrically nonlinear behavior of thin-walled composite box beam.

### Acknowledgments

The support of the research reported here by Korea Ministry of Construction and Transportation through Grant 2006-C106A1030001-06A050300220 and Seoul R&BD Program through Grant GR070033 is gratefully acknowledged.

## APPENDIX A

The explicit forms of the laminate stiffnesses $E_{ij}$ for composite box section in Fig.13 can be defined by

$$\begin{aligned} E_{16} &= (-2x_1 + 2x_p)B_{11}^1 b_1 + D_{11}^1 b_1 + (-2y_2 + 2y_p)B_{11}^2 b_2 + D_{11}^2 b_2 \\ &+ (2x_3 - 2x_p)B_{11}^3 b_1 + D_{11}^3 b_1 + (2y_4 - 2y_p)B_{11}^4 b_2 + D_{11}^4 b_2 \qquad (43a) \\ E_{26} &= (-2x_1 + 2x_p)x_1 B_{11}^1 b_1 + D_{11}^1 (3x_1 - 2x_p)b_1 - F_{11}^1 b_1 \end{aligned}$$

$$
\begin{aligned}
&+ \frac{1}{2}\big[(-2y_2+2y_p)B^2_{11}+D^2_{11}\big]b_2^2+(-2y_2+2y_p)x_1B^2_{11}b_2+D^2_{11}x_1b_2\\
&+ (2x_3-2x_p)x_3B^3_{11}b_1+D^3_{11}(3x_3-2x_p)b_1+F^3_{11}b_1\\
&+ \frac{1}{2}\big[(-2y_4+2y_p)B^4_{11}-D^4_{11}\big]b_2^2+(2y_4-2y_p)x_3B^4_{11}b_2+D^4_{11}x_3b_2 \qquad (43b)\\
E_{36} &= \frac{1}{2}\big[(2x_1-2x_p)B^1_{11}-D^1_{11}\big]b_1^2+(-2x_1+2x_p)y_4B^1_{11}b_1+D^1_{11}y_4b_1\\
&+ (-2y_2+2y_p)y_2B^2_{11}b_2+D^2_{11}(3y_2-2y_p)b_2-F^2_{11}b_2\\
&+ \frac{1}{2}\big[(2x_3-2x_p)B^3_{11}+D^3_{11}\big]b_1^2+(2x_3-2x_p)y_2B^3_{11}b_1+D^3_{11}y_2b_1\\
&+ (2y_4-2y_p)y_4B^4_{11}b_2+D^4_{11}(3y_4-2y_p)b_2+F^4_{11}b_2 \qquad (43c)\\
E_{46} &= \frac{1}{2}\big[(-2x_1+2x_p)A_1B^1_{11}+D^1_{11}(A_1+2x_1-2x_p)-F^1_{11}\big]b_1^2+(-2x_1+2x_p)CB^1_{11}b_1\\
&+ D^1_{11}(C-(-2x_1+2x_p)(-y_4+y_p))b_1-F^1_{11}(-y_4+y_p)b_1\\
&+ \frac{1}{2}\big[(-2y_2+2y_p)A_2B^2_{11}+D^2_{11}(A_2+2y_2-2y_p)-F^2_{11}\big]b_2^2+(-2y_2+2y_p)(A_1b_1+C)B^2_{11}b_2\\
&+ D^2_{11}(A_1b_1+C-(-2y_2+2y_p)(x_1-x_p))b_2-F^2_{11}(x_1-x_p)b_2\\
&+ \frac{1}{2}\big[(2x_3-2x_p)A_3B^3_{11}+D^3_{11}(A_3-2x_3+2x_p)-F^3_{11}\big]b_1^2+(2x_3-2x_p)(A_1b_1+A_2b_2+C)B^3_{11}b_1\\
&+ D^3_{11}(-(2x_3-2x_p)(y_2-y_p)+A_1b_1+A_2b_2+C)b_1-F^3_{11}(y_2-y_p)b_1\\
&+ \frac{1}{2}\big[(2y_4-2y_p)A_4B^4_{11}+D^4_{11}(A_4-2y_4+2y_p)-F^4_{11}\big]b_2^2+(2y_4-2y_p)(C+A_1b_1+A_2b_2+A_3b_1)B^4_{11}b_2\\
&+ D^4_{11}(C+A_1b_1+A_2b_2+A_3b_1-(2y_4-2y_p)(-x_3+x_p))b_2-F^4_{11}(-x_3+x_p)b_2 \qquad (43d)\\
E_{56} &= \frac{1}{2}(-x_1+x_p)\frac{F}{2t_1}B^1_{16}b_1+D^1_{16}(\frac{F}{2t_1}-2x_1+2x_p)b_1+F^1_{16}b_1\\
&+ \frac{1}{2}(-y_2+y_p)\frac{F}{2t_2}B^2_{16}b_2+D^1_{16}(\frac{F}{2t_2}-2y_2+2y_p)b_2+F^2_{16}b_2\\
&+ \frac{1}{2}(x_3-x_p)\frac{F}{2t_3}B^3_{16}b_1+D^3_{16}(\frac{F}{2t_3}+2x_3-2x_p)b_1+F^3_{16}b_1\\
&+ \frac{1}{2}(y_4-y_p)\frac{F}{2t_4}B^4_{16}b_2+D^4_{11}(\frac{F}{2t_4}+2y_4-2y_p)b_2+F^4_{16}b_2 \qquad (43e)\\
E_{66} &= (-4x_1+4x_p)(-x_1+x_p)D^1_{11}b_1+(-4x_1+4x_p)F^1_{11}b_1+H^1_{11}b_1\\
&+ (-4y_2+4y_p)(-y_2+y_p)D^2_{11}b_2+(-4y_2+4y_p)F^2_{11}b_2+H^2_{11}b_2\\
&+ (4x_3-4x_p)(x_3-x_p)D^3_{11}b_1+(4x_3-4x_p)F^3_{11}b_1+H^3_{11}b_1\\
&+ (4y_4-4y_p)(y_4-y_p)D^4_{11}b_2+(4y_4-4y_p)F^4_{11}b_2+H^4_{11}b_2 \qquad (43f)
\end{aligned}
$$

where the St. Venant circuit shear flow $F$, constant $C$ and other values of $E_{ij}$ can be found in Ref.[22].

## APPENDIX B

The element direct stiffness matrix $[K]$ is divided into the linear terms denoted by subscript $L$ and the nonlinear terms denoted by subscript $N$, respectively.

$$[K] = \begin{bmatrix} (K_{ij}^{11})_L & (K_{ij}^{12})_L & (K_{ij}^{13})_L & (K_{ij}^{14})_L \\ & (K_{ij}^{22})_L & (K_{ij}^{23})_L & (K_{ij}^{24})_L \\ & & (K_{ij}^{33})_L & (K_{ij}^{34})_L \\ \text{sym.} & & & (K_{ij}^{44})_L \end{bmatrix} + \begin{bmatrix} (K_{ij}^{11})_N & (K_{ij}^{12})_N & (K_{ij}^{13})_N & (K_{ij}^{14})_N \\ (K_{ij}^{21})_N & (K_{ij}^{22})_N & (K_{ij}^{23})_N & (K_{ij}^{24})_N \\ (K_{ij}^{31})_N & (K_{ij}^{32})_N & (K_{ij}^{33})_N & (K_{ij}^{34})_N \\ (K_{ij}^{41})_N & (K_{ij}^{42})_N & (K_{ij}^{43})_N & (K_{ij}^{44})_N \end{bmatrix} \tag{44}$$

Linear terms of direct stiffness matrix and the force vector are given in Ref.[22]. Nonlinear terms of direct stiffness matrix can be expressed by

$$(K_{ij}^{12})_N = \int_0^l \frac{1}{2}\big[E_{11}(U' + y_p\Phi') - E_{13}\Phi'\big]\Psi_i'\psi_j' dz \tag{45a}$$

$$(K_{ij}^{13})_N = \int_0^l \frac{1}{2}\big[E_{11}(V' - x_p\Phi') + E_{12}\Phi'\big]\Psi_i'\psi_j' dz \tag{45b}$$

$$(K_{ij}^{14})_N = \int_0^l \frac{1}{2}\big[E_{11}(r_p^2\Phi' + y_pU' - x_pV') + E_{12}V' - E_{13}U' + E_{16}\Phi'\big]\Psi_i'\psi_j' dz \tag{45c}$$

$$(K_{ij}^{21})_N = 2K_{ji}^{N,12} \tag{45d}$$

$$\begin{aligned}(K_{ij}^{22})_N &= \int_0^l \frac{1}{2}\big[E_{11}(U' + y_p\Phi')^2 - 2E_{13}(U' + y_p\Phi')\Phi' + E_{33}\Phi'^2\big]\psi_i'\psi_j' dz \\ &- \int_0^l \Big[\frac{1}{2}\big[E_{12}U'' + E_{13}V'' + E_{14}\Phi'' - 2E_{15}\Phi'\big]\psi_i'\psi_j' + \frac{1}{2}\big[E_{12}(U' + y_p\Phi') - E_{23}\Phi'\big](\psi_i''\psi_j' + \psi_i'\psi_j'')\Big] dz\end{aligned} \tag{45e}$$

$$\begin{aligned}(K_{ij}^{23})_N &= \int_0^l \frac{1}{2}\big[E_{11}(V' - x_p\Phi') + E_{12}\Phi'\big](U' + y_p\Phi')\psi_i'\psi_j' - \frac{1}{2}\big[E_{13}(V' - x_p\Phi') + E_{23}\Phi'\big]\Phi'\psi_i'\psi_j' dz \\ &- \int_0^l \Big[\frac{1}{2}\big[E_{12}(V' - x_p\Phi') + E_{22}\Phi'\big]\psi_i''\psi_j' + \frac{1}{2}\big[E_{13}(U' + y_p\Phi') - E_{33}\Phi'\big]\psi_i'\psi_j''\Big] dz\end{aligned} \tag{45f}$$

$$\begin{aligned}(K_{ij}^{24})_N &= \int_0^l \frac{1}{2}\big[(E_{23} - E_{12}y_p)U'' + (E_{33} - E_{13}y_p)V'' + (E_{34} - E_{14}y_p)\Phi''\big]\psi_i'\psi_j' dz \\ &+ \int_0^l \frac{1}{2}\big[E_{11}(r_p^2\Phi' + y_pU' - x_pV') + E_{12}V' - E_{13}U' + E_{16}\Phi'\big](U' + y_p\Phi')\psi_i'\psi_j' dz \\ &- \int_0^l \Big[\frac{1}{2}\big[E_{13}(r_p^2\Phi' + y_pU' - x_pV') + E_{23}V' - E_{33}U' + E_{36}\Phi'\big]\Phi' - \big[E_{15}U' - 2(E_{35} - E_{15}y_p)\big]\Big]\psi_i'\psi_j' dz \\ &- \int_0^l \frac{1}{2}\big[E_{12}(r_p^2\Phi' + y_pU' - x_pV') + E_{22}V' - E_{23}U' + E_{26}\Phi'\big]\Phi'\psi_i''\psi_j' dz \\ &- \int_0^l \frac{1}{2}\big[E_{14}(U' + y_p\Phi') - E_{34}\Phi'\big]\psi_i'\psi_j'' dz\end{aligned} \tag{45g}$$

$$(K_{ij}^{31})_N = 2(K_{ji}^{13})_N \tag{45h}$$

$$(K_{ij}^{32})_N = (K_{ji}^{23})_N \tag{45i}$$

$$(K_{ij}^{33})_N = \int_0^l \frac{1}{2}\big[E_{11}(V' - x_p\Phi')^2 + 2E_{12}(V' - x_p\Phi')\Phi' + E_{22}\Phi'^2\big]\psi_i'\psi_j' dz$$

$$- \int_0^l \Big[\frac{1}{2}\big[E_{12}U'' + E_{13}V'' + E_{14}\Phi'' - 2E_{15}\Phi'\big]\psi_i'\psi_j' + \frac{1}{2}\big[E_{13}(V' - x_p\Phi') + E_{23}\Phi'\big](\psi_i''\psi_j' + \psi_i'\psi_j'')\Big]dz \quad (45j)$$

$$(K_{ij}^{34})_N = \int_0^l -\frac{1}{2}\big[(E_{22} - E_{12}x_p)U'' + (E_{23} - E_{13}x_p)V'' + (E_{24} - E_{14}x_p)\Phi''\big]\psi_i'\psi_j'dz$$
$$+ \int_0^l \frac{1}{2}\big[E_{11}(r_p^2\Phi' + y_pU' - x_pV') + E_{12}V' - E_{13}U' + E_{16}\Phi'\big](V' - x_p\Phi')\psi_i'\psi_j'dz$$
$$+ \int_0^l \Big[\frac{1}{2}\big[E_{12}(r_p^2\Phi' + y_pU' - x_pV') + E_{22}V' - E_{23}U' + E_{36}\Phi'\big]\Phi' + \big[E_{15}V' + 2(E_{25} - E_{15}x_p)\big]\Big]\psi_i'\psi_j'dz$$
$$- \int_0^l \frac{1}{2}\big[E_{13}(r_p^2\Phi' + y_pU' - x_pV') + E_{23}V' - E_{33}U' + E_{36}\Phi'\big]\Phi'\psi_i''\psi_j'dz$$
$$- \int_0^l \frac{1}{2}\big[E_{14}(V' - x_p\Phi') + E_{24}\Phi'\big]\psi_i'\psi_j''dz \quad (45k)$$

$$(K_{ij}^{41})_N = 2(K_{ji}^{14})_N \quad (45l)$$

$$(K_{ij}^{42})_N = (K_{ji}^{24})_N \quad (45m)$$

$$(K_{ij}^{43})_N = (K_{ji}^{34})_N \quad (45n)$$

$$(K_{ij}^{44})_N = \int_0^l \Big[\frac{1}{2}\big[E_{11}(r_p^2\Phi' + y_pU' - x_pV')^2 + E_{22}V'^2 - E_{33}U'^2 + E_{66}\Phi'^2\big] + \big[E_{12}(r_p^2\Phi' + y_pU' - x_pV')V'\big]\Big]\psi_i'\psi_j'dz$$
$$+ \int_0^l \Big[ - E_{13}(r_p^2\Phi' + y_pU' - x_pV')U' - E_{23}U' + E_{16}(r_p^2\Phi' + y_pU' - x_pV')\Phi' + E_{26}\Phi'V' - E_{36}\Phi'U'\Big]\psi_i'\psi_j'dz$$
$$- \int_0^l \frac{1}{2}\big[(E_{26} + E_{12}r_p^2)U'' + (E_{36} + E_{13}r_p^2)V'' + (E_{46} + E_{14}r_p^2)\Phi''\big]\psi_i'\psi_j'dz$$
$$+ \int_0^l \big[2(E_{25} - E_{15}x_p)V' - 2(E_{35} - E_{15}y_p)U' + 3(E_{56} + E_{15}r_p^2)\Phi'\big]\psi_i'\psi_j'dz$$
$$- \int_0^l \frac{1}{2}\big[E_{14}(r_p^2\Phi' + y_pU' - x_pV') + E_{24}V' - E_{34}U' + E_{46}\Phi'\big](\psi_i''\psi_j' + \psi_i'\psi_j'')dz \quad (45o)$$

## References


[1] Vlasov VZ. Thin Walled Elastic Beams, Israel Program for Scientific Translation, Jerusalem, 1961.

[2] Gjelsvik A. The theory of thin-walled bars, New York: John Wiley and Sons Inc., 1981.

[3] Bathe KJ and Bolourchi MS. Large Displacement Analysis of Three-Dimensional Beam Structures. Int J Numer Meth Eng 1979; 14:961-986.

[4] Atilgan AR, Hodges DH. A geometrically nonlinear analysis for nonhomogeneous, anisotropic beams. In: AIAA Paper No.89-1264-CPMobile, AL, Proc. 30th AIAA/ASME/ASCE/ASH/ACS Structures, Structural Dynamics and Materials Conf. 1989, pp.895-908.

[5] Hodges DH, Atilgan AR, Cesnik CES and Fulton MV. On a Simplified Strain Energy Function for Geometrically Nonlinear Behavior of Anisotropic Beams. Compos Eng 1992;2(5-7):513-526.

[6] Cesnik CES and Hodges DH. VABS: A New Concept for Composite Rotor Blade Cross-Sectional Modeling. J Am Helicopter Soc 1997;42(1):27-38.

[7] Cesnik, CES and Shin S. On the modeling of integrally actuated helicopter blades. Int J Solids Struct 2001;38(10-13):1765-1789.

[8] Volovoi VV, Hodges DH, Cesnik CES, Popescu B. Assessment of beam modeling methods for rotor blade applications. Math Comput Model 2001;33(10-11):1099-1112.

[9] Yu W, Hodges DH, Volovoi VV and Fuchs ED. A generalized Vlasov theory for composite beams.Thin-Walled Struct 2005;43(9):1493-1511.

[10] Jeon SM, Cho MH and Lee I. Static and dynamic analysis of composite box beams using large deflection theory. Comput Struct 1995;57(4):635-642.

[11] Bauld NR and Tzeng LS. A Vlasov theory for fiber-reinforced beams with thin-walled open cross section. Int J Solids Struct 1984;20(3):277-297.

[12] Stemple AD and Lee SW. Finite element model for composite beams undergoing large deflection with arbitrary cross sectional warping. Int J Numer Meth Eng 1989;28:2143-2160.

[13] Stemple AD and Lee SW. Large deflection static and dynamic finite element analyses of composite beams with arbitrary cross-sectional warping. In: AIAA Paper No.89-1363-CPMobile, AL, Proc. 30th AIAA/ASME/ASCE/ASH/ACS Structures, Structural Dynamics and Materials Conf. 1989, pp.1788-1798.

[14] Kalfon JP and Rand O. Nonlinear analysis of composite thin-walled helicopter blades. Comput Struct 1993;48(1):51-61.

[15] Pai PF and Nayfeh AH. A fully nonlinear theory of curved and twisted composite rotor blades accounting for warpings and three-dimensional stress effects. Int J Solids Struct 1994;31(9):1309-1340.

[16] Bhaskar K and Librescu L. A geometrically non-linear theory for laminated anisotropic thin-walled beams. Int J Eng Sci 1995;33(9):1331-1344.

[17] Librescu L and Song 0. Thin-walled Composite Beams. The Netherlands: Springer, 2006.

[18] Machado SP and Cortinez VH. Non-linear model for stability of thin-walled composite beams with shear deformation. Thin-Walled Struct 2005;43(10):1615-1645.

[19] Cortinez VH and Piovan MT. Stability of composite thin-walled beams with shear deformability. Comput Struct 2006;84(15-16):978-990.

[20] Machado SP. Geometrically non-linear approximations on stability and free vibration of composite beams. Eng Struct 2007;29:3567-3578.

[21] Lee J. Lateral buckling analysis of thin-walled laminated composite beams with monosymmetric sections. Eng Struct 2006;28(14):1997-2009.

[22] Vo TP and Lee J. Flexural-torsional behavior of thin-walled closed-section composite box beams. Eng Struct

2007;29(8):1774-1782.

[23] Jones RM. Mechanics of composite materials, New York: Hemisphere Publishing Corp., 1975.

[24] Bathe KJ. Finite element procedures, Prentice Hall, 1996.

[25] Lee J. Flexural analysis of thin-walled composite beams using shear-deformable beam theory. Compos Struct 2005;70(2):212-222.

CAPTIONS OF FIGURES

Figure 1: Definition of coordinates and generalized displacements in thin-walled closed sections.

Figure 2: A cantilever composite box beam under a 1.78 kN tip vertical load.

Figure 3: Variation of the vertical displacement with respect to fiber angle change of a cantilever composite box beam under a 1.78 kN tip vertical load.

Figure 4: Variation of the angle of twist with respect to fiber angle change of a cantilever composite box beam under a 1.78 kN tip vertical load.

Figure 5: Variation of axial tip displacement with respect to fiber angle change of a cantilever composite box beam under a 1.78 kN tip vertical load.

Figure 6: Variation of the horizontal displacement with respect to fiber angle change of a cantilever composite box beam under a 1.78 kN tip vertical load.

Figure 7: A pinned-hinged composite box beam under an eccentric uniform load.

Figure 8: Load versus the vertical displacement at mid-span for a pinned-hinged composite box beam under an eccentric uniform load.

Figure 9: Load versus the angle of twist at mid-span for a pinned-hinged composite box beam under an eccentric uniform load.

Figure 10: Load versus the axial displacement at mid-span for a pinned-hinged composite box beam under an eccentric uniform load.

Figure 11: Variation of the vertical and axial displacements at mid-span with respect to fiber angle change for a pinned-hinged composite box beam under an eccentric uniform load.

Figure 12: Variation of the angle of twist at mid-span with respect to fiber angle change for a pinned-hinged composite box beam under an eccentric uniform load.

Figure 13: Geometry of thin-walled composite box section.

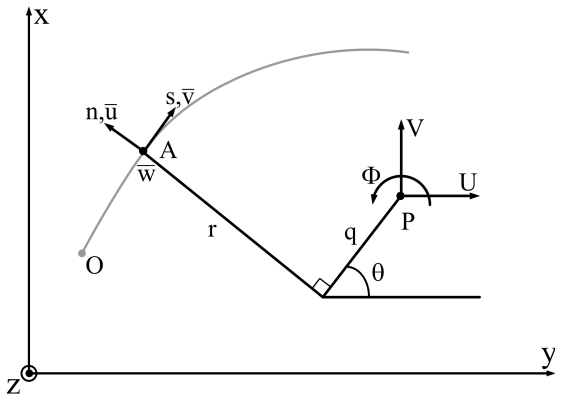


FIG. 1 Definition of coordinates and generalized displacements in thin-walled closed sections.

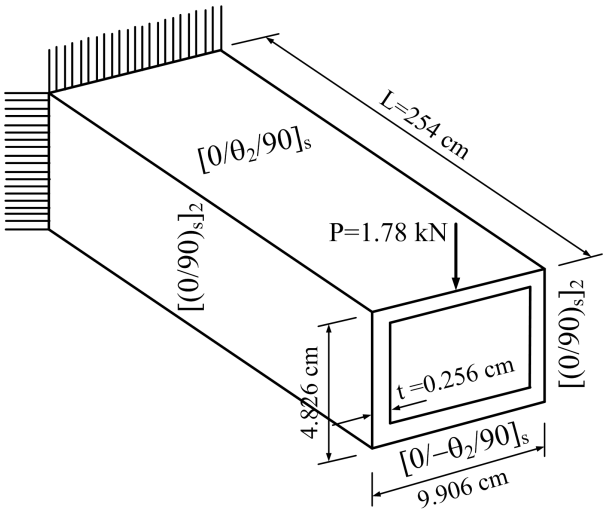


FIG. 2 A cantilever composite box beam under a 1.78 kN tip vertical load

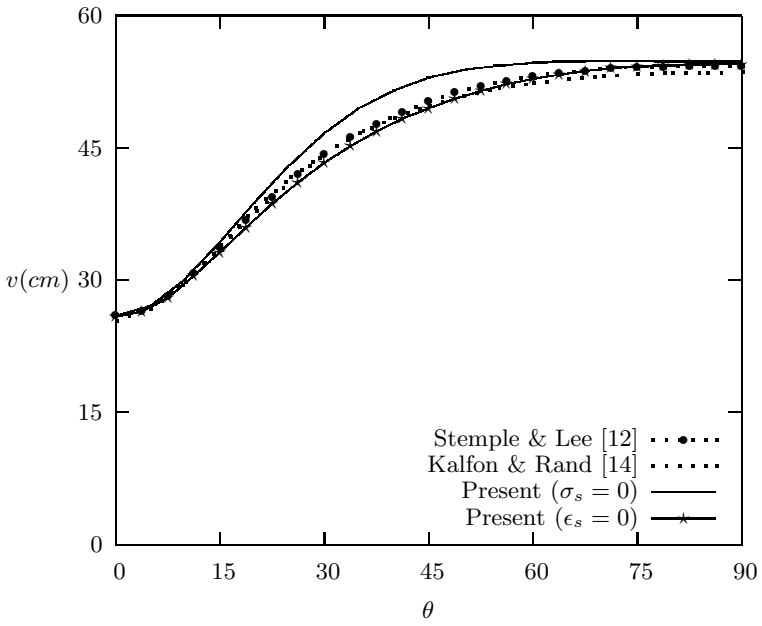


FIG. 3 Variation of the vertical displacement with respect to fiber angle change of a cantilever composite box beam under a 1.78 kN tip vertical load

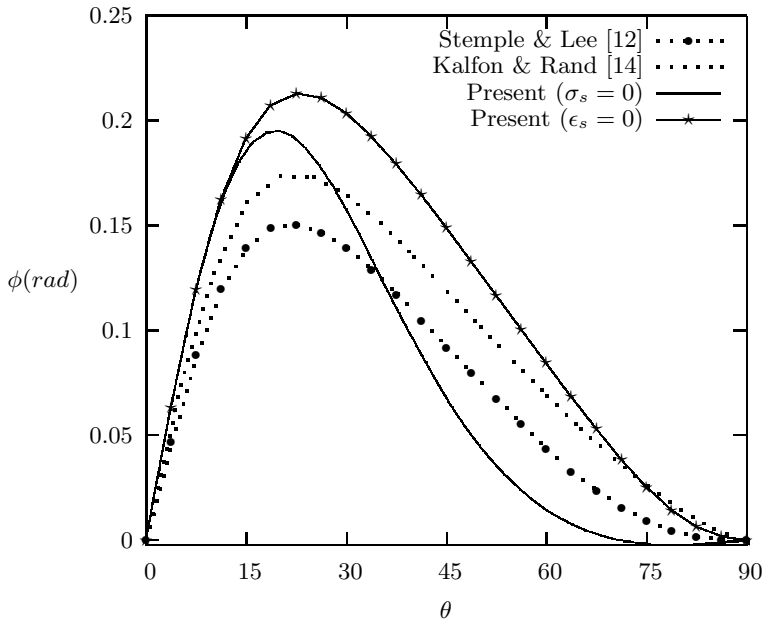


FIG. 4 Variation of the angle of twist with respect to fiber angle change of a cantilever composite box beam under a 1.78 kN tip vertical load

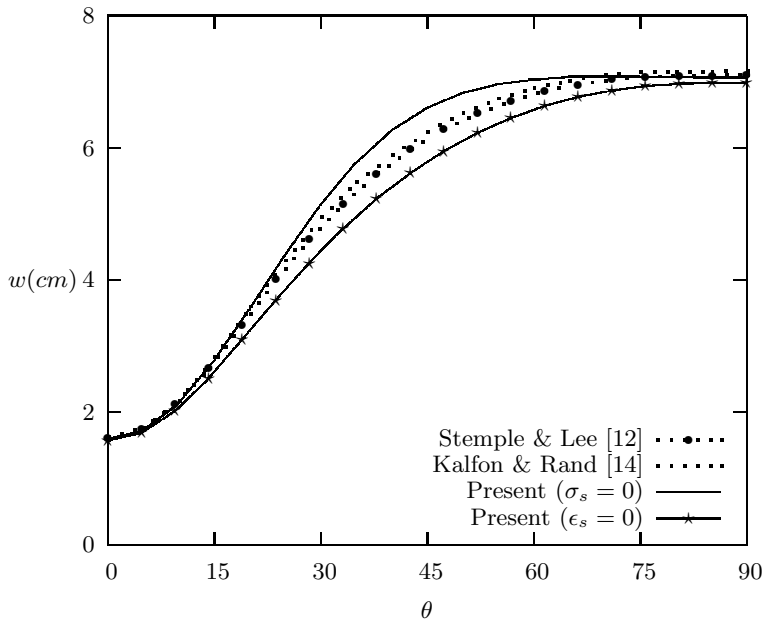


FIG. 5 Variation of axial tip displacement with respect to fiber angle change of a cantilever composite box beam under a 1.78 kN tip vertical load

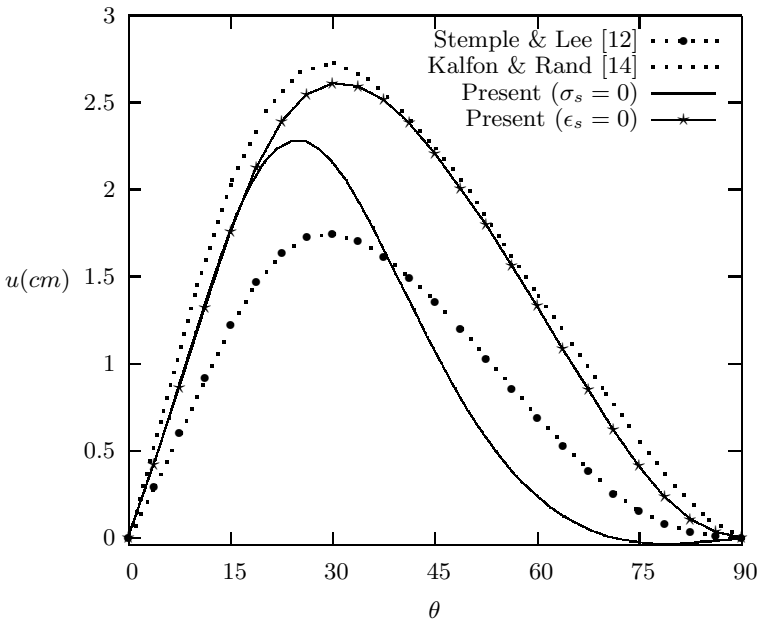


FIG. 6 Variation of the horizontal displacement with respect to fiber angle change of a cantilever composite box beam under a 1.78 kN tip vertical load

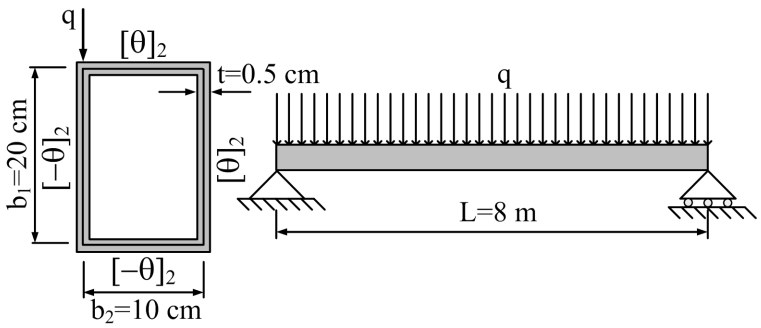


FIG. 7 A pinned-hinged composite box beam under an eccentric uniform load

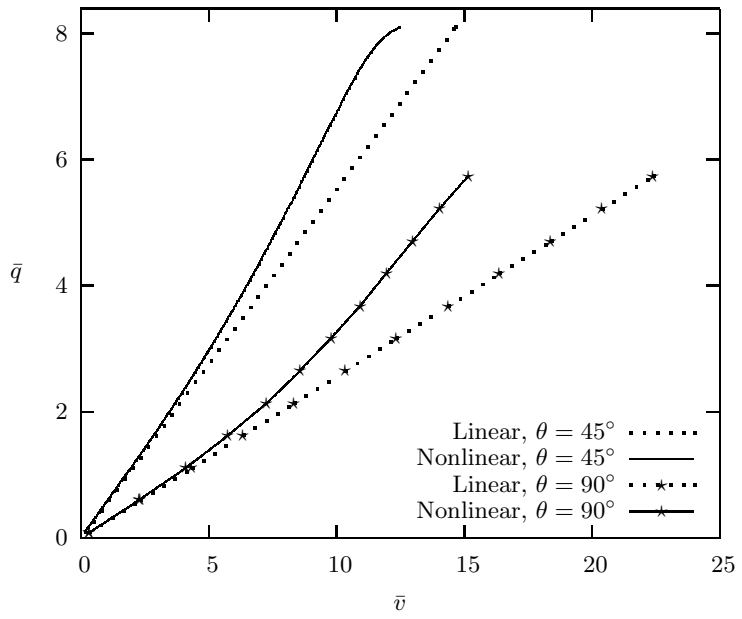


FIG. 8 Load versus the vertical displacement at mid-span for a pinned-hinged composite box beam under an eccentric uniform load

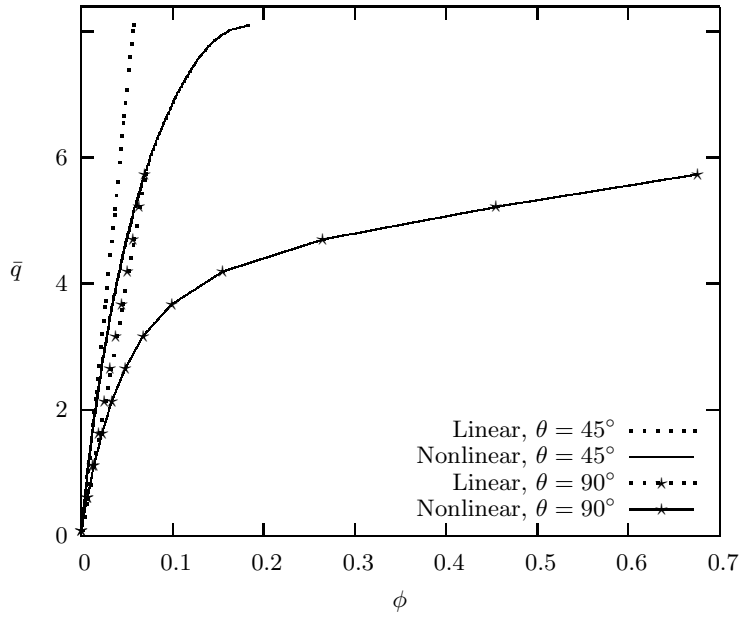


FIG. 9 Load versus the angle of twist at mid-span for a pinned-hinged composite box beam under an eccentric uniform load

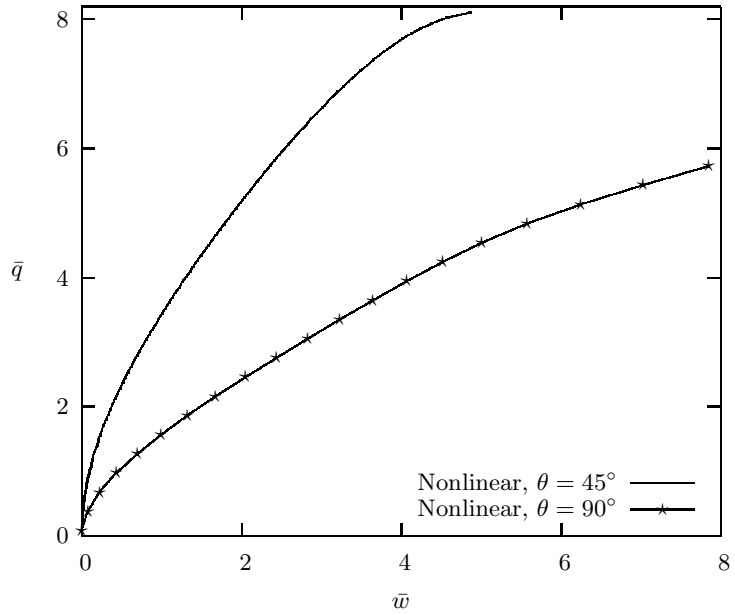


FIG. 10 Load versus the axial displacement at mid-span for a pinned-hinged composite box beam under an eccentric uniform load

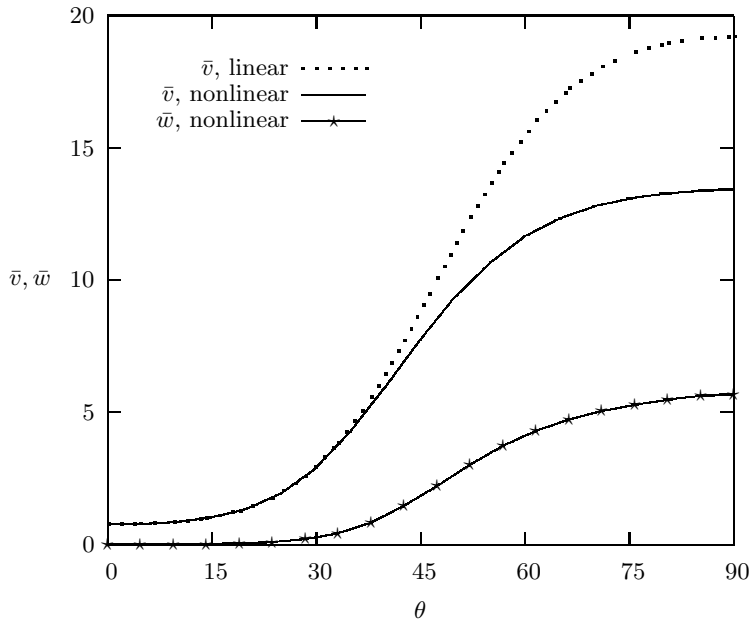


FIG. 11 Variation of the vertical and axial displacements at mid-span with respect to fiber angle change for a pinned-hinged composite box beam under an eccentric uniform load

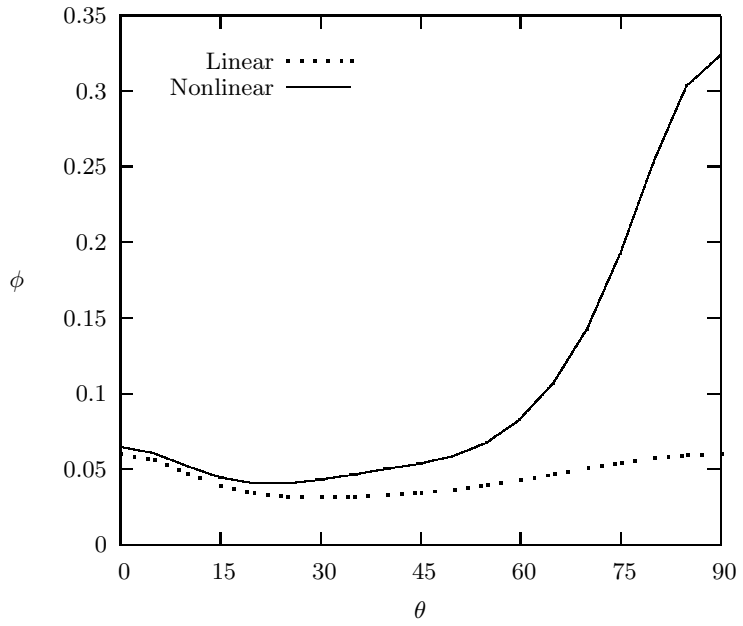


FIG. 12 Variation of the angle of twist at mid-span with respect to fiber angle change for a pinned-hinged composite box beam under an eccentric uniform load

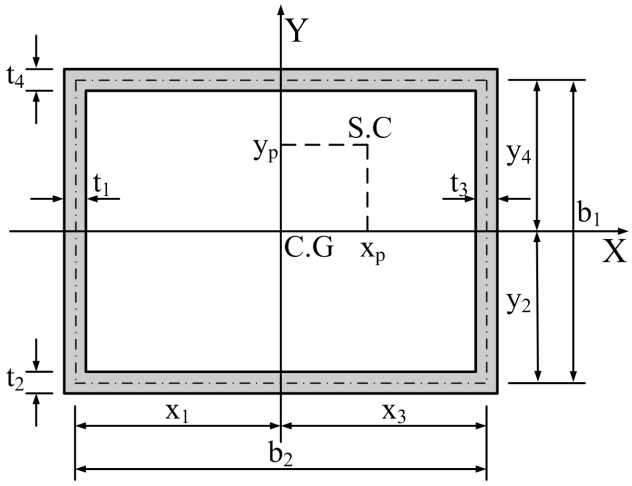


FIG. 13 Geometry of thin-walled composite box section

**SEJONG UNIVERSITY**
*Department of Architectural Engineering*

June 2, 2008

Professor K.J. Bathe,
Department of Mechanical Engineering,
Massachusetts Institute of Technology, Cambridge, MA 02139-4307, USA

Dear Professor K.J. Bathe:

Subject: TECHNICAL PAPER SUBMIT

Enclosed is electronic copy of a manuscript by Thuc Phuong Vo and myself entitled "Geometrically nonlinear analysis of thin-walled composite box beams", which I would like to consider for publication in the ***Computers & Structures***. This manuscript has not been previously published, nor has it been submitted elsewhere for consideration.

Should you have a question concerning this matter, please make all correspondence to me.

Sincerely,

Professor Jaehong Lee

98 KUNJA DONG, KWANGJIN KU • SEOUL • 143-747• KOREA
PHONE: 82-2-3408-3287 • FAX: 82-2-3408-3331 • E-MAIL: jhlee@sejong.ac.kr